African Journal of Biological Sciences

Journal homepage: http://www.afjbs.com

Research Paper   **Open Access**

An optimization of synthesis parameters for Faujasite zeolite-X using Response Surface Methodology conjunction with Central Composite Design

Divya Tirva[1], Dharmesh Sur[1*,]Kaushal Agheda[2]

[1]Department of Chemical Engineering, Faculty of Technology,
Marwadi University, Rajkot 360003, Gujarat, India.
[2]Department of Applied Physics, Faculty of Technology and Engineering

Abstract:

The study assesses the feasibility of using Class C coal fly ash (CFA) to produce faujasite zeolite-X materials. This study primarily investigated the production and analysis of zeolites using coal fly ash (CFA) as a starting material. The authors have utilized the response surface methodology combined with central composite design approach to optimize the process variables. The examined operational parameters include fusion temperature, fusion time, liquid/solid (L/S) ratio, alkaline solution concentration and hydrothermal treatment time. The investigation revealed that samples were produced from three highly efficient reactions that took place under the following conditions: The NaOH/fly ash ratio for each of the three reactions was 1.5 and 1.75 respectively. The fusion temperature for all three reactions was 675°C, with a fusion time of 12-15 hours and a reaction time of 8 hours. The most superior zeolite materials were analyzed for their mineralogical properties using X-ray powder diffraction (XRD), scanning electron microscopy-energy-dispersive X-ray spectroscopy (SEM-EDS), BET surface analysis (for pore volume and pore width) and chemical composition using X-ray fluorescence (XRF). The findings obtained were comparable to the zeolite structures derived from coal fly ash. Thus, it can be inferred that the examined coal fly ash has the potential to serve as a suitable medium for the production of faujasite type zeolite materials. The XRF analysis validates the composition of the fly ash and the resulting Faujasite, consistent with prior findings and an enhanced composition. The surface area analyses (BET) revealed that the synthesized Faujasite has an active area of 1080 m^2g^{-1} with pore volume of 0.662406 cm³/g and pore diameter 24.486 Å, whereas the fly ash only has an area of 60 m^2g^{-1} for its physicochemical qualities. Meanwhile, the EDX analysis combined with SEM confirmed that the composition of the samples aligns with the desired outcomes and that the proposed methodology is supported by the observed morphological characteristics.

Keywords: Faujasite Zeolite-X; Alkaline Fusion Hydrothermal Treatment; Design of experiment; Response surface methodology; Central Composite Design

1. Introduction

The rapid growth of the economy and dependence on primary energy sources has had a negative influence on all parts of the environment. In 2023, the worldwide demand for coal rose by around 1.5%, reaching a total of over 4.7 billion tonnes. In March 2023, China and India achieved significant milestones in their respective coal production. China exceeded 400 million tonnes, marking the second occurrence of such an achievement. Meanwhile, India

surpassed 100 million tonnes for the first time in history. The surge was propelled by a 1% upsurge in power generation and a 2% growth in non-power industrial uses. The global disposal of coal fly ash (CFA) from coal-based power plants is a widespread and significant issue (Gollakota et al., 2020; Asl et al., 2018; Seidler et al., 2020). The Third Amendment Notification, issued by the Ministry of Environment, Forests, and Climate Change of the Government of India on January 25, 2016, restricts the dumping and disposal of fly ash in order to protect valuable land. In order to attain a state of zero waste, it is imperative to fully use 100% of the fly ash that is produced. The cement industry only utilizes the first and second grades of fly ash, which constitute 63% of the total fly ash production (Rastogi et al., 2020). The remaining waste is discarded in ash ponds. According to the estimate, our annual coal consumption is projected to exceed 1.8 billion metric tons by the year 2032. (Surabhi, 2017). Indian coal has an ash content ranging from 35% to 45%, with occasional instances where it exceeds 50% (Ahmed et al., 2016). According to Jindal 2019, coal-based thermal power stations now create over 197 million metric tonnes of coal ash per year. By 2032, this number is projected to increase to roughly 600 million metric tons yearly. In order to reduce the pozzolanic properties of fly ash, a conventional method of disposal is used, which involves disposing of fly ash slurries. This disposal technique necessitates a substantial amount of land, spanning thousands of hectares, as well as an immense volume of water, totaling in the billions of cubic meters, on an annual basis. Due to its environmental impact, it needs careful consideration. The present investigation is focused on the process of alkaline fusion hydrothermal synthesis of Faujasite type Na-X zeolite using material obtained from an Indian thermal power plant. The prospective investigation utilized a range of analytical techniques to compare the synthesized zeolite with the reference commercially available zeolite. Emphasizing the attainment of a high level of crystallinity was given priority. The objective of synthesizing the zeolite Na-X using fly ash as a cost-effective adsorbent was to effectively capture and remove dye waste wastewater generated by the local textile industry.

2. Experiment

2.1 Materials

The CFA was obtained from the coal-fired thermal power plant situated in Kutch, Gujarat, India. Table 2 presents the chemical composition of the untreated fly ash obtained from the power plant site. The XRF analysis indicates that the composition of CFA is mostly SiO_2 and Al_2O_3, making it well-suited for research and the production of adsorbents. Sodium aluminate has been acquired from Shreekala Pvt. Ltd. located in Vadodara, Gujarat. HCL (Merk) and NaOH (Merk) were used to carry out alkaline and acidic treatments, respectively.

2.2 Synthesis

Prior to processing, the fly ash samples underwent a thorough filtration using a BSS Tyler screen featuring an 80-mesh aperture, which effectively eliminated sizable particles. Through a calcination process lasting three hours at 800°C, unburned carbon (3-6%) and additional volatile substances are eliminated from fly ash. To facilitate the development of zeolite crystallisation, fly ash samples were subjected to treatment with 2.5 M HCL (Tirva, D 2023; Ojha et al. 2004). The development and proliferation of zeolite crystals are impeded by iron. This occurs due to the precipitate of iron, which results in the formation of iron hydroxide and a decrease in the OH-ion concentration. The formation of zeolites is significantly reliant on the existence of OH-ions. The coal fly ash to sodium hydroxide ratio

varied between 1 and 2. The calcined and HCl-treated fly ash was incorporated with sodium hydroxide in a predetermined quantity. Following this, the mixture was pulverised and fused for two hours at temperatures spanning from 550 to 700°C in a stainless steel container. Sodium aluminate was incorporated in the form of a seeding agent. Following the mixture's cooling to room temperature, it was pulverised and incorporated into distilled water at a concentration of 10 g CFA per 100 ml water. The constituents were heated for a period of 18 hours at a temperature of 90°C to facilitate their preparation for hydrothermal treatment. Once the precipitate underwent desiccation at 800 °C, it was filtered to a pH of less than 10, and any residual sodium hydroxide was removed by repeatedly rinsing it with distilled water.

2.3 Design of experiment

The optimization of process conditions was achieved through the utilisation of Stat-ease Design Expert (version 10.1). In conjunction with central composite design (CCD), response surface methodology (RSM) was utilised to determine the optimal reaction parameters (temperature, concentration, adsorbent dosage, and reaction time) for maximal crystallinity of faujasite zeolite-X. RSM utilises statistical techniques to analyse the behaviour of a data set by fitting experimental data with a polynomial equation [27]. The adequacy of the derived model was subsequently assessed using diagnostic analysis of variance (ANOVA) tests [28]. Equation (1) was utilised to depict the fitting of the experimental response data to a second-order polynomial model.

$$Y = \beta_0 + \sum_{i=1}^{k} \beta_i x_i + \sum_{i=1}^{k} \beta_{ii} x_i^2 + \sum_{i=1} 1 \sum_{i=1} \beta_{ij} x_i x_j + \varepsilon$$

……….Eq (1)

The experimental procedure employed the following representations of the independent factors xi and xj: where 0 represents the constant coefficient, i and ii denote the linear and quadratic coefficients, respectively, ij represents the interaction coefficient, and represents the residual error. The solutions obtained for the regression equation represented two-dimensional contour plots and coefficients. The interrelation between the variables can be deduced through an analysis of the two-dimensional outline graphs that are presented within the specified interval. Through the implementation of a desirability function, both the response's requirements and individual factors were concurrently guaranteed. In order to establish a quantitative correlation between variables and multiple responses, RSM employs an assortment of mathematical and statistical methods. At five levels, variables are assessed in the RSM based on the central composite design (CCD). Low levels (-) and high levels (+) are entered by the operator into the software, which then generates additional levels.

Result and Discussion

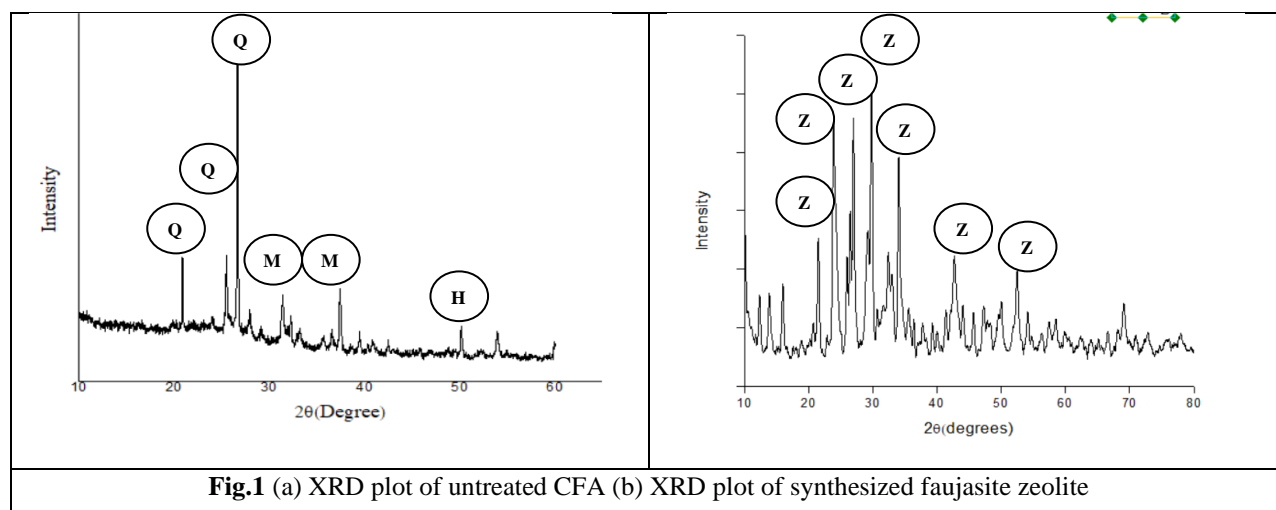### 3.1 Adsorbent characterization

X- Ray Fluorescence

Table 1 displays the zeolite that is derived from the unprocessed CFA, along with an analysis of the material compositions. The legitimacy of the CFA study's classification as class F type (Ojha et al. 2004; Boycheva et al. 2020) is substantiated by the observation that the cumulative proportions of SiO_2, Al_2O_3, and Fe_2O_3 surpass 70%, while CaO remains under 20%. The coal fly ash consists mostly of SiO2 and Al2O3, with a ratio of 1.92 (SiO_2 to

Al_2O_3). The XRF examination uncovers the mineral composition of the unmodified sample, which is appropriate for the production of zeolite. Jha et al. (2009) and Chigondo and Nyamunda (2013) provide corroborating evidence for this claim. Therefore, CFA may be considered a viable and cost-effective primary material in the production of zeolite. The particles, ranging in size from 0.1nm to 1.2nm, were mostly elliptical or circular in form. During the alkaline fusion hydrothermal treatment, sodium ions (Na+) are introduced into the zeolite framework. Analysis shows that the Na_2O oxide content of the synthesised product increases from 1.88% to 15.60%. (2009, Jha et al.)

Table 1 XRF analysis of the CFA

Oxides	Composition (wt. %) of fly ash	Composition (wt. %) of Faujasite Zeolite-X
Sodium oxide	2.07	16.70
Magnesium oxide	0.82	0.78
Aluminum oxide	29.65	29.80
Silicon dioxide	52.30	50.01
Phosphorus pentoxide	0.25	0.02
Ferric oxide	9.62	0.73
Sulfur trioxide	0.28	0.12
Potassium oxide	0.68	2.33
Calcium oxide	1.68	5.58
Titanium dioxide	1.72	0.6
Chromic Oxide	0.09	0.06

X- Ray Diffraction

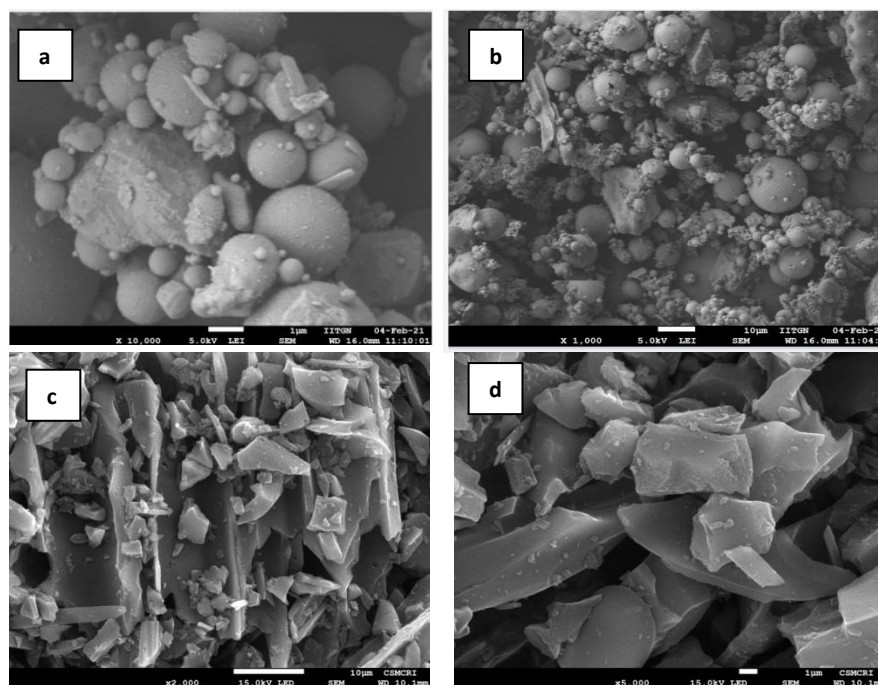**Fig.1** (a) XRD plot of untreated CFA (b) XRD plot of synthesized faujasite zeolite

The Philips X'pert MPD XRD equipment at CSMCRI Bhavnagar was used to get XRD patterns from CFA and synthesised faujasite zeolite-X. The powdered materials were subjected to scanning and analysis throughout the range of 10o and 60o (2Ө, representing the angle of diffraction). Crystallinity was assessed by calculating the total area beneath the most prominent peaks in XRD patterns. Figure 3 illustrates the X-ray diffraction (XRD) properties of both CFA and the resulting faujasite zeolite-X, which was created by alkaline fusion hydrothermal treatment.

Coal fly ash is mostly composed of silica, alumina, and magnetite, as well as oxides of magnesium, calcium, phosphorus, and titanium. The unmodified fly ash consisted of quartz (SiO_2 at 26.85º) and mullite ($Al_2O_3.SiO_2$), together with tiny amounts of hematite and magnetite (Tirva, D 2023; Ojha et al. 2004). Based on the CFA analysis, the samples consist predominantly of an amorphous phase. The XRD analysis provides empirical evidence of the existence of a glass phase in CFA, as shown by a prominent peak seen throughout the angular range of 16º to 36º. The X-ray diffraction (XRD) plot indicates higher intensities in the hydrothermally synthesized products, potentially resulting from a greater concentration of faujasite zeolite-X (Kunecki et al., 2017). Sharp peaks are indicative of the existence of a crystalline phase.

Scanning Electron Microscopy

The JEOL JSM 7100F device was used to examine the structure of CFA and produce zeolite using a scanning electron microscope. The SEM/EDAX analysis was used to estimate the fraction of oxides in both CFA and the resulting zeolite, based on their bulk and elemental contents. Scanning electron microscope pictures of the treated coal fly ash offer additional proof of the alkaline fusion hydrothermal technique's success in transforming fly ash into crystalline Faujasite-type zeolite-X. The synthesized adsorbent has exhibited a notable level of crystallinity, as seen in the studies conducted by Nawagamuwa and Wijesooriya (2018), Jha et al. (2009), and Chigondo et al. (2013). The predominant minerals identified in the Class F category of CFA utilized in this investigation include quartz, mullite, and hematite. Before the hydrothermal procedure, iron oxide was extracted from CFA using HCl. The morphologies of CFA and faujasite zeolite-X were observed using FE-SEM investigation (Fig. 3). The presence of amorphous CFA is shown by the spherical formations seen in Figure 3 (a) and (b). Figure 3 (c and d) demonstrates that zeolite-X, belonging to the Faujasite class, generated angular crystal formations.
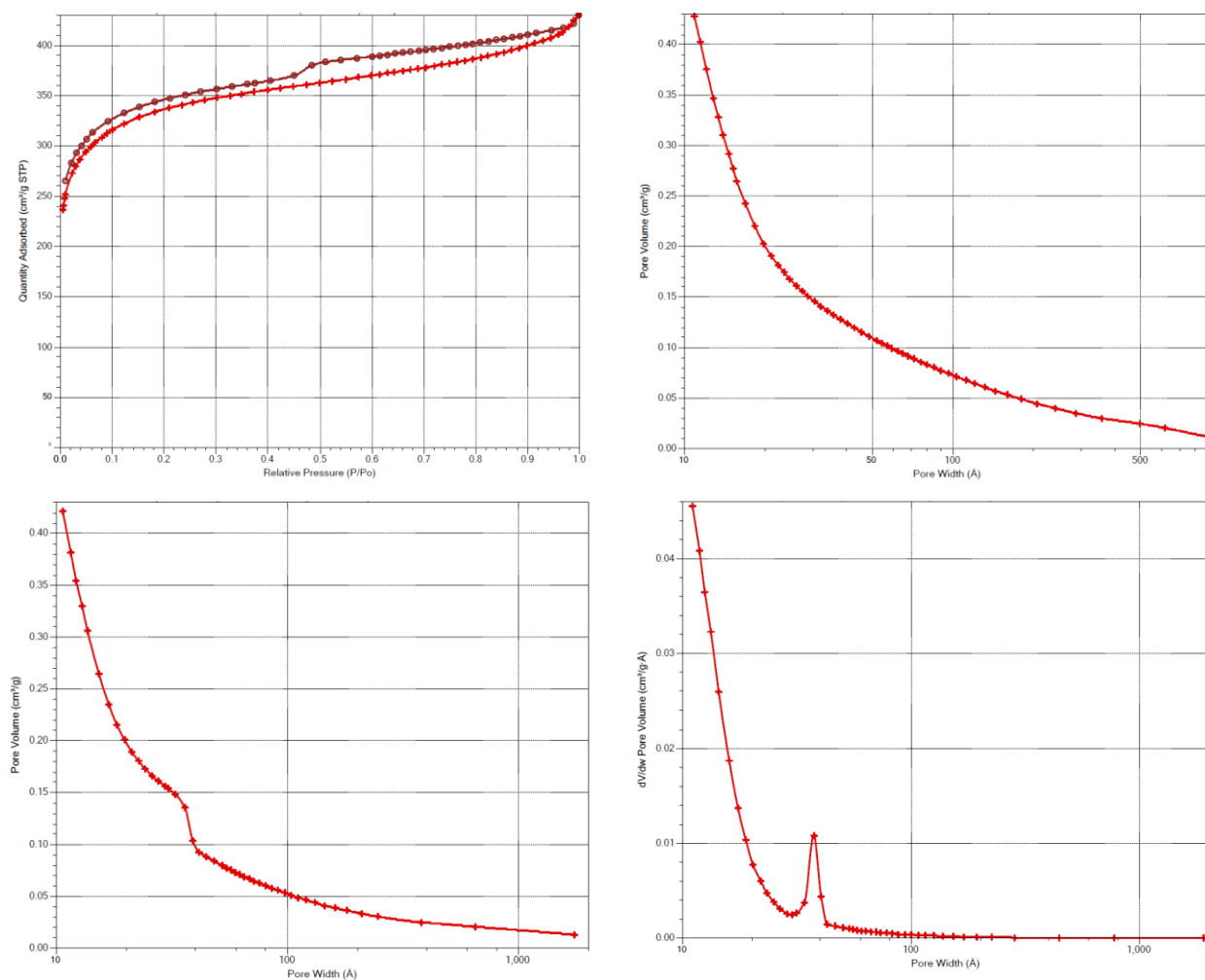
Fig. 2 SEM graphics of coal fly ash (a), (b) and synthesised fujasite
zeolite-X (c), (d)

BET surface area analysis

The samples were tested using nitrogen adsorption at a temperature of 196.15 °C. Before conducting the analyses, the samples were subjected to degassing in a vacuum at a temperature of 105 °C for duration of 12 hours. The specific surface area was determined using the Brunauer-Emmett-Teller (BET) technique.

Table 2 BET surface analysis

1)	Pore size(nm)	0.662406 cm³/g
2)	Specific surface area(m²/g)	1080 m²g⁻¹
3)	Pore volume(cm³/g)	0.662406 cm³/g

Fig. 3 (a) Isotherm Linear Plot (b) BJH Adsorption dV/dw Pore Volume (c) BJH Desorption Cumulative Pore Volume (Larger) and (d) BJH Desorption dV/dw Pore Volume

The specific amounts and range of the independent variables used in the central composite design (CCD) are outlined in Table 2. The experiment will utilize a set of five independent variables: Fusion temperature (ºC) (A), Fusion time (h) (B), NaOH (C), (D) L/S ratio (mg/L), and Hydrothermal treatment time (E). The results of the experiment's 32 trials are displayed in Table 5, along with the percentage of crytallinity of synthesized zeolite. By utilizing the CCD design and doing analysis of variance (ANOVA), it was feasible to predict the interaction. Equation (5) represents the percentage of crytallinity of synthesized zeolite using a coded equation, where ò represents the values of independent and interacting factors.

% Crystallinity of faujasite zeolite-X = 95.56 +1.44*A + 0.2625*B + 1.34*C + 0.0758*D + 0.0550*E - 0.1000*AB - 0.0400*AC - 0.0737*AD + 0.1150*AE - 0.1062*BC - 0.0025*BD + 0.2337*BE + 0.0075*CD - 0.0838*CE - 0.2025*DE - 0.3778*A² - 0.2928*B² - 0.4328 C² - 0.3441*D² - 0.4291*E²............ Eq. (2)

Table 4 shows that the model's F-Value is 669.39, indicating its significance. Given that each factor has a "Prob>F" value below 0.05, all of them may be considered statistically significant. The presence of a non-significant lack of fit (2.04) offers more confidence in the adequacy of the mathematical equations fit. The Pred R-Squared value (0.9873) is in close proximity to the Adj R-Squared value (0.9935). Adeq Precision greater than 4 signifies a suitable signal.

Table 3 Range and levels of variables

Independent variables	Variables range and levels			
	1	**2**	**3**	**4**
(A) Fusion Temperature (^{0}C)	550	600	650	700
(B) Fusion Time (h)	9	12	15	18
(C) NaOH (M)	1	1.5	2	2.5
(D) L / S Ratio (mg/L)	1.1	1.3	1.5	1.7
(E) Hydrothermal treatment time	4	6	8	10

Table 4 Analysis of Variance (ANOVA) results for Synthesis to the zeolite

Source	Sum of Squares	df	Mean Square	F-value	p-value	
Model	112.79	20	0.56	227.16	<0.001	significant
A-Fusion Temperature (^{0}C)	49.42	1	4.94	1993.42	<0.001	
B-Fusion Time (h)	1.65	1	0.16	66.78	<0.001	
C-NaOH (M)	43.26	1	4.32	1745.12	<0.001	
D-L / S Ratio (mg/L)	0.138	1	0.01	5.57	0.008	
E-Hydrothermal treatment time	0.07	1	0.07	2.93	< 0.0001	
AB	0.16	1	0.01	6.45	<0.001	
AC	0.02	1	0.02	1.03	<0.001	
AD	0.08	1	0.08	3.51	<0.001	
AE	0.21	1	0.02	8.53	<0.001	
BC	0.18	1	0.01	7.29	<0.001	
BD	0.00	1	0.00	0.01	<0.001	
BE	0.87	1	0.08	35.26	<0.001	
CD	0.00	1	0.00	0.04	<0.001	
CE	0.11	1	0.01	4.53	<0.001	

DE	0.65	1	0.06	26.46	<0.001	
A²	4.19	1	0.41	169.01	<0.001	
B²	2.52	1	0.25	101.34	<0.001	
C²	5.50	1	0.55	222.12	<0.001	
D²	3.47	1	0.35	14.68	<0.001	
E²	5.40	1	0.54	218.56	<0.001	
Residual	27.27	11	0.25			
Lack of Fit	27.02	6	4.51	2.04	<0.0001	significant
Pure Error	0.25	5	0.05			
Cor Total	140.07	31				

Summary of quadratic model

Response	Mean	SD	R^2		Adj-R^2	Pred-R^2	CV %	AP
% CV	94.15	0.15	0.9980		0.9935	0.9873	0.167	5.232

df: degrees of freedom, CV %: coefficient of variation, SD: standard deviation, R:regression coefficient, AP: adequate precision.
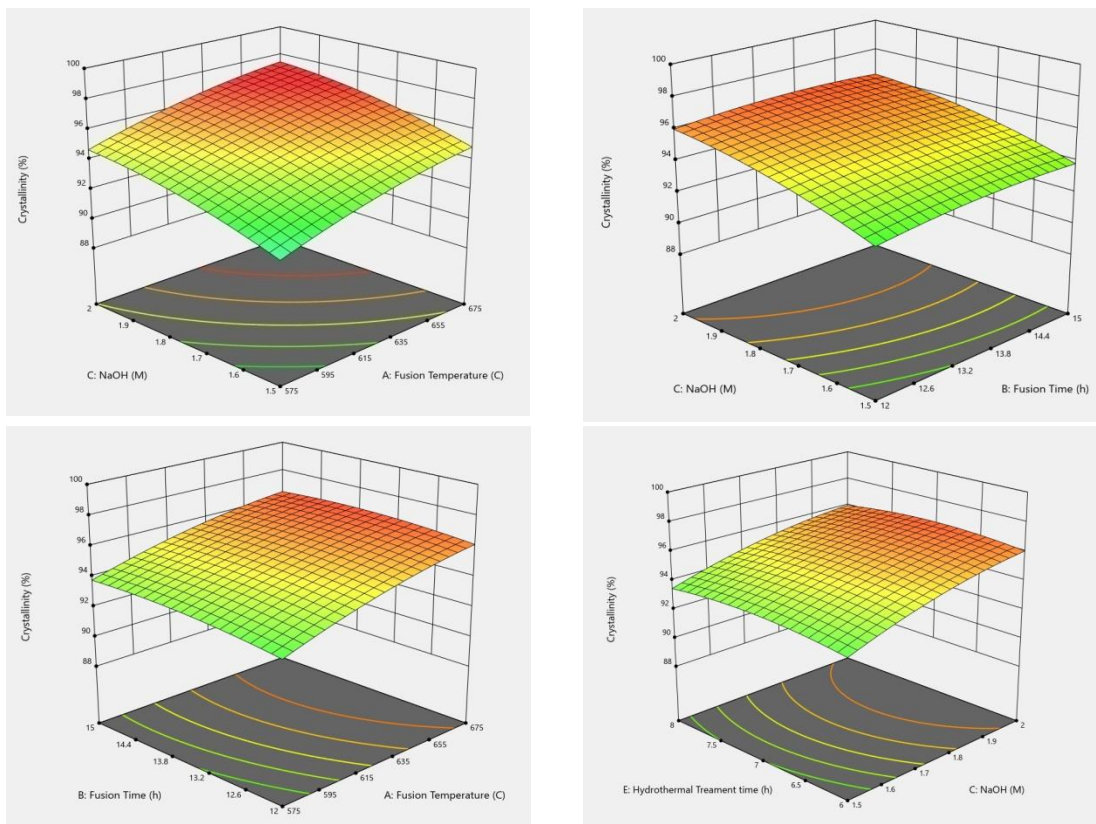
Table 5 Comparison of Experimental and Predicted results							
Run	A	B	C	D	E	EXP	PRE
1	675	15	1.5	1.5	6	93.27	93.36
2	675	12	1.5	1.3	6	92.24	92.56
3	675	15	2	1.5	8	96.76	96.98
4	625	13.5	1.75	1.2	7	95.59	95.25
5	625	13.5	1.75	1.4	7	95.74	95.26
6	625	16.5	1.75	1.4	7	95.26	95.46
7	625	13.5	1.75	1.4	9	94.37	94.76
8	625	13.5	1.75	1.4	7	94.69	95
9	675	12	1.5	1.5	8	92.92	92.8
10	625	13.5	1.25	1.4	7	93.89	93.57
11	575	12	2	1.3	6	92.19	92.69
12	525	13.5	1.75	1.4	7	93.37	93.47
13	575	15	1.5	1.5	8	90.12	90.57
14	575	15	1.5	1.3	6	89.84	89.57
15	575	12	1.5	1.5	6	89.23	89.65
16	625	13.5	1.75	1.4	7	94.37	94.89
17	575	15	2	1.5	6	93.46	93.79
18	625	13.5	1.75	1.4	5	94.69	94.97
19	625	13.5	1.75	1.4	7	95.78	95.34
20	575	15	2	1.3	8	93.16	93.67
21	675	15	1.5	1.3	8	94.60	94.36
22	675	12	2	1.5	6	96.18	96.76
23	575	12	1.5	1.3	8	89.36	88.95
24	625	13.5	2.25	1.4	7	96.37	96.13
25	625	13.5	1.75	1.4	7	95.75	95.35
26	625	13.5	1.75	1.6	7	94.98	95.16
27	625	10.5	1.75	1.4	7	95.28	95.36

28	625	13.5	1.75	1.4	7	95.85	95.47
29	575	12	2	1.5	8	92.74	92.46
30	675	13.5	1.75	1.4	7	96.26	96.67
31	675	12	2	1.3	8	96.17	96.45
32	675	15	2	1.3	6	95.68	96.12

3.2 Response surface methodology

Figure 4 exhibits many three-dimensional contour plots illustrating the correlation between two variables and the percentage of crystallinity of fujasite zeolite-X. These graphs provide a visual representation of the statistical impact of the parameter settings. Figure 4 (a) demonstrates the collective influence of NaOH and Fusion temperature. It is evident that raising both the concentration and fusion temperature led to a rise in crystallinity. Figure 4 (b) illustrates the collective influence of NaOH and Fusion time on the percentage of crystallinity. An increase in the concentration of NaOH resulted in a proportional increase in the structure of zeolite. Furthermore, when the Fusion time continued to increase, there was a notable rise in crystallinity, but soon it started to decline. Nevertheless, a notable surge has been noticed as a result of the extension of Fusion time from 9 hours to 15 hours. The NaOH/fly ash ratio, also known as the L/S ratio, plays a crucial role in the synthesis process. This is because the addition of Na+ ions helps in the creation of the basic unit structure. An exponential shift in zeolite crystallinity has been reported within the range of 1.1 to 1.75 L/S ratio. Concentration is of utmost importance in the process of alkaline fusion synthesis. The observations were made in the plot depicted in Figure 4 (d) and Figure 4 (g).

Fig 4. Simultaneous effects of (a) NaOH and Fusion temperature (b) NaOH and Fusion time (c) Fsuion time and Fusion temperature, (d) Hydrothermal treatment time and NaOH (e) Hydrothermal treatment time and Fusion temperature (f) Hydrothermal treatment time and Fusion time (g) L/S ratio and NaOH (h) L/S ratio and Fusion temperature (i) L/S ratio Fusion time (j) Hydrothermal treatment time and L/S ratio on the percentage of crytallinity of synthesized zeolite are illustrated using contour plots

Conclusion

The initial substance utilized in this investigation is the byproduct of thermal power plants. This study primarily focuses on the sustainability approach. The process of hydrothermal alkaline treatment was employed to produce an adsorbent based on coal fly ash (CFA), namely Faujasite Zeolite-X. The RSM +CCD approach was used to analyse

the impact of fusion temperatures, fusion time, NaOH concentrations, hydrothermal treatment time and L/S ratios on the crystallization of synthesized zeolite. The anticipated quantity of faujasite zeolite-X was employed to ascertain a response parameter. In our investigation of zeolite crystallization, we utilized X-ray diffraction (XRD), X-Ray Fluorescence (XRF) and scanning electron microscopy with energy-dispersive X-ray spectroscopy (SEM-EDX). The chemical and morphological properties of fly ash have changed, indicating its transformation into zeolite materials. The creation of zeolitic material was highly dependent on the ratio of the raw material and the circumstances of treatment. Through manipulation of the reaction conditions, zeolites with different surface area, silica/alumina ratio, and crystallinity were produced. Optimal surface area and highest crystallinity were achieved using the following conditions: A solution with a sodium hydroxide (NaOH) concentration of 2 M was used, with a NaOH to fly ash ratio of 1:5. The fusion temperature was set at 675 K, and the mixture was aged for 15 hours. Following this, a hydrothermal treatment was carried out for 8 hours. The resulting structure was found to be similar to that of commercial zeolite 13X.

Below is a brief summary of the results obtained by analyzing the XRD, IR, and SEM data of the Na-X type zeolite synthesized by activating fly ash sourced from an Indian thermal power plant:

1. An ideal temperature of 675 degrees Celsius has been established for manufacturing 72% crystalline zeolite Faujasite Zeolite-X. In their study, Bai et al. (2018) discovered that a significantly elevated fusion temperature is essential to induce the dissolution of quartz into soluble silicon. It was observed that raising the temperature from more than 700°C led to the deformation and depletion of these minerals. Quartz was shown to undergo full conversion into soluble material when exposed to a temperature of 650 degrees Celsius, as evidenced by the absence of diffraction peaks. Guozhi et al. (2019) found that the temperature at which alkali fusion takes place affects the production of zeolite. It has been discovered that increasing the fusion temperature causes the activation of inert compounds found in fly ash, such as quartz, mullite, corundum, and others. The diffraction strength at the peak gradually increases, suggesting a growth in the crystallinity of the zeolite.

2. The NaOH to fly ash (L/S) ratio is a crucial determinant in the zeolitization process. Elevating the sodium content in the reactant mixture will result in a greater production of sodium silicates that are soluble in water. In subsequent stages, the synthesis of sodium silicates escalates, leading to a greater output of zeolitic substances. Additionally, the Na+ cation plays a crucial role in the zeolitization process. Observations have revealed that sodium ions have a role in stabilizing the constituent units of zeolite frameworks, specifically the six-membered ring. The stability is essential for the formation of zeolite in hydrothermal environments (Ojha et al., 2004). The ANOM investigation demonstrates that the crystallinity of zeolite shows an increasing pattern as the concentration of NaOH rises up to 2 M, but thereafter undergoes a gradual decrease.

3. Fly ash contains many other constituents that are undesirable in the production of zeolites, apart from SiO_2 and Al_2O_3. The acid treatment process employed during pre-treatment efficiently eliminates many unwanted contaminants from the resulting zeolite, including iron (III) oxide, calcium oxide, and magnesium oxide. These contaminants can hinder the process of crystallization. The current work utilized

hydrochloric acid (HCl) to decrease the concentrations of iron and alkali oxides found in fly ash. Natush and Taylor reported in 1980 that the co ntaminants were primarily found in the outer layer of the ash particles.

Future Scope

The purpose of this research is to develop an adsorbent (Faujasite zeolite-X) for the treatment of dye-waste effluent in the common effluent treatment plant (CETP) of the Rajkot district (Gujarat-India), which manages over 200 small and medium-scale industrial enterprises (4 common effluent treatment plants). This work suggests the economic viability of treating waste effluent in the CETP by substituting activated carbon with the synthesized zeolite for adsorption treatment (during secondary treatment).

Author's contributions

DT: Performing the experiments, data collection and analysis, first draft of manuscript. **DS**: Review and editing of manuscript, Communications. **KA**: Performing design of experiments

Acknowledgement

References

1) Ahmed, S., Saurikhia, A., Haleem, A., and Gangopadhyay, S. (2016). Geographical spread of fly ash generation and residual potential for its utilization in India. *Int. J. Innov. Res. Rev*, *4*(1), 8-19. https://doi.org/10.1016/j.jhazmat.2007.05.071

2) Alpat SK , Ozbayrak O , Alpat S , Akcay H . The adsorption kinetics and removal of cationic dye, toluidine blue o, from aqueous solution with Turkish zeolite. J Hazard Mater 2008;151:213–20

3) Amodu OS , Ojumu TV , Ntwampe SK , Ayanda OS . Rapid adsorption of crystal violet onto magnetic zeolite synthesized from fly ash and magnetite nanoparticles. J Encapsul Adsorption Sci 2015;5:191–203. DOI: 10.4236/jeas.2015.54016

4) Asl, S. M. H., Ghadi, A., Baei, M. S., Javadian, H., Maghsudi, M., andKazemian, H. (2018). Porous catalysts fabricated from coal fly ash as cost-effective alternatives for industrial applications: a review. *Fuel*, *217*, 320-342. DOI: https://doi.org/10.1016/j.fuel.2017.12.111

5) Astuti, W., Chafidz, A., Wahyuni, E. T., Prasetya, A., Bendiyasa, I. M., and A based, A. E. (2019). Methyl violet dye removal using coal fly ash (CFA) as a dual sites adsorbent. *Journal of Environmental Chemical Engineering*, *7*(5), 103262. DOI: https://doi.org/10.1016/j.jece.2019.103262

6) Alam, J., and Akhtar, M. N. (2011). Fly ash utilization in different sectors in Indian scenario. *Int J Emerg Trends Eng Dev*, *1*(1), 1-14

Divya Tirva / Afr.J.Bio.Sc. 6(9) (2024)

7) Al-dahri, T., AbdulRazak, A. A., andRohani, S. (2020). Preparation and characterization of Linde-type A zeolite (LTA) from coal fly ash by microwave-assisted synthesis method: its application as adsorbent for removal of anionic dyes. *International Journal of Coal Preparation and Utilization*, 1-14. DOI: https://doi.org/10.1080/19392699.2020.1792456

8) Bayat, M., Nabavi, M. S., and Mohammadi, T. (2018). An experimental study for finding the best condition for PHI zeolite synthesis using Taguchi method for gas separation. *Chemical Papers*, *72*, 1139-1149. DOI: https://doi.org/10.1007/s11696-017-0366-6

9) Bhimani, H. B. (2011). *Bacterial degradation of Azo Dyes and its derivatives* (Doctoral dissertation, Saurashtra University).

10) Bonetti, B., Waldow, E. C., Trapp, G., Hammercshmitt, M. E., Ferrarini, S. F., Pires, M. J., ... and Aquino, T. F. (2021). Production of zeolitic materials in pilot scale based on coal ash for phosphate and potassium adsorption in order to obtain fertilizer. Environmental Science and Pollution Research, 28(3), 2638-2654. DOI: https://doi.org/10.1007/s11356-020-11447-y

11) Boycheva, S., Marinov, I., Miteva, S., andZgureva, D. (2020). Conversion of coal fly ash into nanozeolite Na-X by applying ultrasound assisted hydrothermal and fusion-hydrothermal alkaline activation. *Sustainable Chemistry and Pharmacy*, *15*, 100217. DOI: https://doi.org/10.1016/j.scp.2020.100217

12) Brião, G. V., Jahn, S. L., Foletto, E. L., & Dotto, G. L. (2018). Highly efficient and reusable mesoporous zeolite synthetized from a biopolymer for cationic dyes adsorption. *Colloids and Surfaces A: Physicochemical and Engineering Aspects*, *556*, 43-50. https://doi.org/10.1016/j.colsurfa.2018.08.019

13) Castro, P. R. D. S. D., Maia, A. Á. B., & Angélica, R. S. (2020). Study of the thermal stability of faujasite zeolite synthesized from kaolin waste from the Amazon. *Materials Research*, *22*, e20190321. DOI: https://doi.org/10.1590/1980-5373-MR-2019-0321

14) Charnell, J. F. (1971). Gel growth of large crystals of sodium A and sodium X zeolites. *Journal of crystal growth*, *8*(3), 291-294. DOI: https://doi.org/10.1016/0022-0248(71)90074-1

15) Chakraborty S , Chowdhury S , Das Saha P . Adsorption of crystal violet from aqueous solution onto NaOH-modified rice husk. Carbohydr Polym 2011;86: 1533–41. DOI: https://doi.org/10.1016/j.carbpol.2011.06.058

16) Chigondo, M., and Nyamunda, B. (2013). Synthesis and characterization of zeolites from coal fly ash (CFA).

17) Cunico P, Kumar A , Fungaro DA. Adsorption of dyes from simulated textile wastewater onto modified nanozeolite from coal fly ash. J Nanosci Nano eng 2015;1:148–61.

18) Cundy, C. S., and Cox, P. A. (2005). The hydrothermal synthesis of zeolites: Precursors, intermediates and reaction mechanism. *Microporous and mesoporous materials*, *82*(1-2), 1-78. DOI: https://doi.org/10.1016/j.micromeso.2005.02.016

19) Dabrowski A. Adsorption—from theory to practice. Adv Colloid Interface Sci 2001; 93:135–224.

20) Deng, L., Xu, Q., and Wu, H. (2016). Synthesis of zeolite-like material by hydrothermal and fusion methods using municipal solid waste fly ash. *Procedia Environmental Sciences*, *31*, 662-667. DOI: https://doi.org/10.1016/j.proenv.2016.02.122

21) Ding, L., Zheng, Y., Hong, Y., and Ring, Z. (2007). Effect of particle size on the hydrothermal stability of zeolite beta. *Microporous and mesoporous materials*, *101*(3), 432-439. DOI: https://doi.org/10.1016/j.micromeso.2006.12.008

22) Derkowski, A., Franus, W., Beran, E., and Czímerová, A. (2006). Properties and potential applications of zeolitic materials produced from fly ash using simple method of synthesis. *Powder technology*, *166*(1), 47-54. DOI: https://doi.org/10.1016/j.powtec.2006.05.004

23) Ferreira, B. C. S., Teodoro, F. S., Mageste, A. B., Gil, L. F., de Freitas, R. P., & Gurgel, L. V. A. (2015). Application of a new carboxylate-functionalized sugarcane bagasse for adsorptive removal of crystal violet from aqueous solution: kinetic, equilibrium and thermodynamic studies. *Industrial Crops and Products*, *65*, 521-534. https://doi.org/10.1016/j.indcrop.2014.10.020

24) Fly Ash Management: Legal Requirements and Other Issues by Ministry of Environment, Forests and Climate Change Government of India., (2019). DOI: https://missionenergy.org/flyash2019/presentations/MoEF.pdf

25) Flanigen EM , Khatami H , Szymanski HA . Infrared structural studies of zeolite frameworks. Mol Sieve Zeolites-I 1974; Chapter 6:201–229. Flanigen E.M et al. 1974. 10.1021/ba-1971-0101.ch016

26) Fungaro, D. A., Bruno, M., and Grosche, L. C. (2009). Adsorption and kinetic studies of methylene blue on zeolite synthesized from fly ash. Desalination and Water Treatment, 2(1-3), 231-239.

27) Furness, E. (1996). Engineering Methods for Robust Product Design: Using Taguchi Methods in Technology and Product Development. *Quality Progress*, *29*(6), 125.

28) Ghaedi M , Ansari A , Habibi MH , Asghari AR . Removal of malachite green from aqueous solution by zinc oxide nanoparticle loaded on activated carbon: kinetics and isotherm study. J Ind Eng Chem 2014; 20:17–28 .

29) Gross-Lorgouilloux, M., Soulard, M., Caullet, P., Patarin, J., Moleiro, E., & Saude, I. (2010). Conversion of coal fly ashes into faujasite under soft temperature and pressure conditions: Influence of additional silica. *Microporous and Mesoporous Materials*, *127*(1-2), 41-49. DOI: https://doi.org/10.1016/j.micromeso.2009.06.026

30) Gupta N , Kushwaha AK , Chattopadhyaya MC . Adsorption studies of cationic dyes onto Ashoka (Saraca asoca) leaf powder. J Taiwan Inst Chem Eng 2012;43:604–13. DOI: https://doi.org/10.1016/j.jtice.2012.01.008

31) Gollakota, A. R., Volli, V., Munagapati, V. S., Wen, J. C., and Shu, C. M. (2020). Synthesis of novel ZSM-22 zeolite from Taiwanese coal fly ash for the selective separation of Rhodamine 6G. *Journal of Materials Research and Technology*, *9*(6), 15381-15393 DOI: https://doi.org/10.1016/j.jmrt.2020.10.070

Divya Tirva / Afr.J.Bio.Sc. 6(9) (2024)

32) Gücek, A., Şener, S., Bilgen, S., & Mazmancı, M. A. (2005). Adsorption and kinetic studies of cationic and anionic dyes on pyrophyllite from aqueous solutions. *Journal of colloid and interface science*, *286* (1) , 53-60. DOI: https://doi.org/10.1016/j.jcis.2005.01.012

33) Holler, H. and Wirsching, U. (1985) Zeolite Formation from Fly Ash. Fortschritte der Mineralogie, 63, 21-43.

34) Ho, K. Y., McKay, G., & Yeung, K. L. (2003). Selective adsorbents from ordered mesoporous silica. *Langmuir*, *19*(7), 3019-3024.
DOI: https://doi.org/10.1021/la0267084

35) Harja, M., Buema, G., Sutiman, D., and Cretescu, I. (2013). Removal of heavy metal ions from aqueous solutions using low-cost sorbents obtained from ash. *Chemical Papers*, *67*(5), 497-508. DOI: https://doi.org/10.2478/s11696-012-0303-7

36) Han R , Wang Y , Zou W , Wang Y , Shi J . Comparison of linear and non- linear analysis in estimating the Thomas model parameters for methylene blue adsorption onto natural zeolite in fixed-bed column. J Hazard Mater 2007; 145: 331–5. DOI: https://doi.org/10.1016/j.jhazmat.2006.12.027

37) He H , Yang S , Yu K , Ju Y , Sun C , Wang L . Microwave induced catalytic degra- dation of crystal violet in nano-nickel dioxide suspensions. J Hazard Mater 2010; 173:393–400. DOI: https://doi.org/10.1016/j.jhazmat.2009.08.084

38) Ho YS . Isotherms for the sorption of lead onto peat: comparison of linear and non-linear methods. Polish J Environ Stud 2006;15:81–6.

39) Iqbal, A., Sattar, H., Haider, R., andMunir, S. (2019). Synthesis and characterization of pure phase zeolite 4A from coal fly ash. *Journal of Cleaner Production*, *219*, 258-267. DOI: https://doi.org/10.1016/j.jclepro.2019.02.066

40) Jha, V. K., Nagae, M., Matsuda, M., and Miyake, M. (2009). Zeolite formation from coal fly ash and heavy metal ion removal characteristics of thus-obtained Zeolite X in multi-metal systems. *Journal of environmental management*, *90*(8), 2507-2514. DOI: https://doi.org/10.1016/j.jenvman.2009.01.009

41) Karadag D , Akgul E , Tok S , Erturk F , Kaya MA , Turan M . Basic and reactive dye removal using natural and modified zeolites. J Chem Eng Data 2007; 52: 2436–41 .

42) Kunecki, P., Panek, R., Wdowin, M., & Franus, W. (2017). Synthesis of faujasite (FAU) and tschernichite (LTA) type zeolites as a potential direction of the development of lime Class C fly ash. *International Journal of Mineral Processing*, *166*, 69-78. DOI: https://doi.org/10.1016/j.minpro.2017.07.007

43) Kumar R, Ahmad R . Biosorption of hazardous crystal violet dye from aqueous solution onto treated ginger waste (TGW). Desalination 2011; 265:112–18. DOI: https://doi.org/10.1016/j.desal.2010.07.040

44) Kumar, S., Upadhyay, S. N., & Upadhya, Y. D. (1987). Removal of phenols by adsorption on fly ash. *Journal of Chemical Technology & Biotechnology*, *37*(4), 281-290. DOI: https://doi.org/10.1002/jctb.280370408

45) Klunk, M. A., Schröpfer, S. B., Dasgupta, S., Das, M., Caetano, N. R., Impiombato, A. N., and Moraes, C. A. M. (2020). Synthesis and characterization of mordenite zeolite from metakaolin and rice husk ash as a

source of aluminium and silicon. *Chemical Papers*, *74*, 2481-2489. DOI: https://doi.org/10.1007/s11696-020-01095-4

46) Kumar, Vimal., Ananda kumar, R., and Mathur, M. U. K. E. S. H. (2003). Management of fly ash in India: a perspective. DOI: https://www.osti.gov/etdeweb/biblio/20371407

47) Labik, L. K., Kwakye-Awuah, B., Abavare, E. K. K., Sefa-Ntiri, B., Nkrumah, I., and Williams, C. (2020). Adsorption Characteristics of Zeolite A Synthesized from Wassa Kaolin for Thermal Energy Storage. *Journal of Materials Science Research*, *9*(3), 1-21. DOI: http://hdl.handle.net/123456789/14752

48) Lin, C. F., and Hsi, H. C. (1995). Resource recovery of waste fly ash: synthesis of zeolite-like materials. *Environmental science and technology*, *29*(4), 1109-1117. DOI: https://doi.org/10.1021/es00004a033

49) Lin, J. X., Zhan, S. L., Fang, M. H., Qian, X. Q., & Yang, H. (2008). Adsorption of basic dye from aqueous solution onto fly ash. *Journal of Environmental Management*, *87*(1), 193-200. https://doi.org/10.1016/j.jenvman.2007.01.001

50) Makgabutlane, B., Nthunya, L. N., Nxumalo, E. N., Musyoka, N. M., and Mhlanga, S. D. (2020). Microwave irradiation-assisted synthesis of zeolites from coal fly ash: An optimization study for a sustainable and efficient production process. *ACS omega*, *5*(39), 25000-25008. DOI: https://doi.org/10.1021/acsomega.0c00931

51) Mafi Gholami R , Mousavi SM , Borghei SM . Process optimization and mod- eling of heavy metals extraction from a molybdenum rich spent catalyst by aspergillus niger using response surface methodology. J Ind Eng Chem 2012;18: 218–24 DOI: https://doi.org/10.1016/j.jiec.2011.11.006

52) Mittal A , Mittal J , Malviya A , Kaur D , Gupta VK . Adsorption of hazardous dye crystal violet from wastewater by waste materials. J Colloid Interface Sci 2010; 343: 463–73.DOI: https://doi.org/10.1016/j.jcis.2009.11.060

53) Mittal, H., Babu, R., Dabbawala, A. A., Stephen, S., & Alhassan, S. M. (2020). Zeolite-Y incorporated karaya gum hydrogel composites for highly effective removal of cationic dyes. *Colloids and Surfaces A: Physicochemical and Engineering Aspects*, *586*, 124161.DOI: https://doi.org/10.1016/j.colsurfa.2019.124161

54) Mohan D, Singh KP, Singh G , Kumar K . Removal of dyes from wastewater using flyash, a low-cost adsorbent. Ind Eng Chem Res 2002;41: 3688–95. DOI: https://doi.org/10.1021/ie010667

55) Momina, Rafatullah, M., Ismail, S., & Ahmad, A. (2019). Optimization study for the desorption of methylene blue dye from clay based adsorbent coating. *Water*, *11*(6), 1304. https://doi.org/10.3390/w11061304

56) Monash P, Pugazhenthi G . Adsorption of crystal violet dye from aqueous solu- tion using mesoporous materials synthesized at room temperature. Adsorption 2009; 15:390–405. DOI: https://doi.org/10.1007/s10450-009-9156-y

57) Mondal, P., Baksi, S., & Bose, D. (2017). Study of environmental issues in textile industries and recent wastewater treatment technology. *World Scientific News*, *61*(2), 98-109.

58) Muthukumaran C , Sivakumar VM , Thirumarimurugan M .Adsorption isotherms and kinetic studies of crystal violet dye removal from aqueous solution using surfactant modified magnetic nanoadsorbent. J Taiwan Inst Chem Eng 2016;63:354–62 . DOI: https://doi.org/10.1016/j.jtice.2016.03.034

59) Nawagamuwa, U. P., and Wijesooriya, N. (2018). Use of flyash to improve soil properties of drinking water treatment sludge. *International Journal of Geo-Engineering*, *9*(1), 3.

60) Ndlovu, N. Z., Missengue, R. N., Petrik, L. F., & Ojumu, T. (2017). Synthesis and characterization of faujasite zeolite and geopolymer from South African coal fly ash. *Journal of Environmental Engineering*, *143*(9), 04017042. DOI: https://doi.org/10.1061/(ASCE)EE.1943-7870.0001212

61) Ojha, K., Pradhan, N. C., and Samanta, A. N. (2004). Zeolite from fly ash: synthesis and characterization. Bulletin of Materials Science, 27(6), 555-564.

62) Pathak, C. Y., Roy, D., and Das, S. (2014). Utilization of fly ash by product in synthetic zeolites. World Journal of Civil Engineering and Construction Technology, 1(1), 002- 0011.

63) Park, S. H., and Park, S. H. (1996). Robust design and analysis for quality engineering (Vol. 20). London: Chapman and Hall.

64) Parra-Huertas, R. A., Calderón-Carvajal, C. O., Gómez-Cuaspud, J. A., & Vera-López, E. (2023). Synthesis and characterization of Faujasite-Na from fly ash by the fusion-hydrothermal method. Boletín de la Sociedad Española de Cerámica y Vidrio, 62(6), 527-542.

DOI: https://doi.org/10.1016/j.bsecv.2023.01.004

65) Querol, X., Umana, J. C., Plana, F., Alastuey, A., Lopez-Soler, A., Medinaceli, A., and Garcia-Rojo, E. (2001). Synthesis of zeolites from fly ash at pilot plant scale. Examples of potential applications. Fuel, 80(6), 857-865.

66) Rastogi, A., and Paul, V. K. (2020). A critical review of the potential for fly ash utilisation in construction-specific applications in India. *Environmental Research, Engineering and Management*, *76*(2), 65-75.

67) Ren, X., Qu, R., Liu, S., Zhao, H., Wu, W., Song, H., and Gao, X. (2020). Synthesis of zeolites from coal fly ash for the removal of harmful gaseous pollutants: A review. *Aerosol and Air Quality Research*, *20*(5), 1127-1144.

68) Saeed A , Sharif M , Iqbal M . Application potential of grapefruit peel as dye sor- bent: kinetics, equilibrium and mechanism of crystal violet adsorption. J Hazard Mater 2010;179:564–72 .DOI: https://doi.org/10.1016/j.jhazmat.2010.03.041

69) Salahshoor Z ,Shahbazi A . Modeling and optimization of cationic dye adsorption onto modified SBA-15 by application of response surface methodology. Desalin Water Treat 2016; 57:1–17 DOI: https://doi.org/10.1080/19443994.2015.1060537

70) Sari A, Mendil D , Tuzen M , Soylak M . Biosorption of Cd(II) and Cr(III) from aqueous solution by moss (Hylocomium splendens) biomass: equilibrium, kinetic and thermodynamic studies. Chem Eng J 2008; 144:1–9 DOI: https://doi.org/10.1016/j.cej.2007.12.020

71) Seidler, Maria, and Malloy, Ken. A Comprehensive Survey of Coal Ash Law and Commercialization: Its Environmental Risks, Disposal Regulation, and Beneficial Use Markets. United States. DOI: https://doi.org/10.2172/1869929

72) Sivalingam S , Sen S . Optimization of synthesis parameters and characterization of coal fly ash derived nano-crystalline mesoporous zeolite x. Appl Surf Sci 2018; 455:903–10. https://doi.org/10.1016/j.jtice.2018.10.032

73) Sivalingam, S., and Sen, S. (2019). Efficient removal of textile dye using nanosized fly ash derived zeolite-x: kinetics and process optimization study. *Journal of the Taiwan Institute of Chemical Engineers*, *96*, 305-314. https://doi.org/10.1016/j.jtice.2018.10.032 (Sivalingam. S and Sujit S 2019)

74) Supelano, G. I., Cuaspud, J. G., Moreno-Aldana, L. C., Ortiz, C., Trujillo, C. A., Palacio, C. A., ... and Gómez, J. M. (2020). Synthesis of magnetic zeolites from recycled fly ash for adsorption of methylene blue. Fuel, 263, 116800. DOI: https://doi.org/10.1016/j.fuel.2019.116800

75) Shukla, S. P., and Mohan, D. (2019). Management of Coal Fly Ash in Remediation Process. In *Innovation in Global Green Technologies 2020*. IntechOpen.

76) Srivastava, V. C., Mall, I. D., and Mishra, I. M. (2007). Multicomponent adsorption study of metal ions onto bagasse fly ash using Taguchi's design of experimental methodology. *Industrial and Engineering Chemistry Research*, *46*(17), 5697-5706. DOI: https://doi.org/10.1021/ie0609822

77) Sun Z , Li C , Wu D . Removal of methylene blue from aqueous solution by ad- sorption onto zeolite synthesized from coal fly ash and its thermal regenera- tion. J Chem Technol Biotechnol 2010; 85:845–50. DOI: https://doi.org/10.1002/jctb.2377

78) Sudha, G., Subramanian, E., & Murugan, C. (2015). Development of iron oxide/zeo-NaX nano photocatalyst from coal fly ash and its activity assessment by methylene blue dye degradation. *International Research Journal of Natural and Applied Sciences*, *2*, 114-28.

79) Surabhi, S. (2017). Fly ash in India: generation vis-à-vis utilization and Global perspective. *Int J Appl Chem*, *13*(1), 29-52.

80) Tan, I. A. W., Hameed, B. H., & Ahmad, A. L. (2007). Equilibrium and kinetic studies on basic dye adsorption by oil palm fibre activated carbon. *Chemical engineering journal*, *127*(1-3), 111-119. DOI: https://doi.org/10.1016/j.cej.2006.09.010

81) Tirva, D., Palkar, R. R., & Agheda, K. (2023). An optimization of synthesis technique for Na-X zeolite from coal-fly ash using Taguchi experimental design. *Chemical Papers*, 1-11.

82) The Gazette of India dated JANUARY 27, 2016 , MINISTRY OF ENVIRONMENT, FORESTS AND CLIMATE CHANGE NOTIFICATION, New Delhi, the 25th January, 2016

83) Wang, Y., Lv, T., Ma, Y., Tian, F., Shi, L., Liu, X., andMeng, C. (2016). Synthesis and characterization of zeolite L prepared from hydrothermal conversion of magadiite. *Microporous and Mesoporous Materials*, *228*, 86-93. https://doi.org/10.1016/j.micromeso.2016.03.028

84) Xiao M , Hu X , Gong Y , Gao D , Zhang P , Liu Q , et al. Solid transformation syn- thesis of zeolites from fly ash. RSC Adv 2015; 5: 100743–9. https://doi.org/10.1039/C5RA17856H

85) Xie, J., Wang, Z., Wu, D., & Kong, H. (2014). Synthesis and properties of zeolite/hydrated iron oxide composite from coal fly ash as efficient adsorbent to simultaneously retain cationic and anionic pollutants from water. *Fuel*, *116*, 71-76. https://doi.org/10.1016/j.fuel.2013.07.126

86) Yousuf, A., Manzoor, S. O., Youssouf, M., Malik, Z. A., and Khawaja, K. S. (2020). Fly ash: production and utilization in India-an overview. *J Mater Environ Sci*, *11*(6), 911-921.

87) Zhou, K., Zhang, Q., Wang, B., Liu, J., Wen, P., Gui, Z., & Hu, Y. (2014). The integrated utilization of typical clays in removal of organic dyes and polymer nanocomposites. *Journal of Cleaner Production*, *81*, 281-289. DOI: https://doi.org/10.1016/j.jclepro.2014.06.038   (Zhou et al. 2014)

88) Zhou, C., Gao, Q., Luo, W., Zhou, Q., Wang, H., Yan, C., & Duan, P. (2015). Preparation, characterization and adsorption evaluation of spherical mesoporous Al-MCM-41 from coal fly ash. *Journal of the Taiwan institute of chemical engineers*, *52*, 147-157. 038 DOI: https://doi.org/10.1016/j.jtice.2015.02.